

1 Published in Transportation Research Record, Journal of the Transportation Research Board,  
2 No. 2290, Concrete Materials 2012, 139-146, 2012.

3  
4  
5  
6  
7  
8 Reducing Set Retardation in High Volume Fly Ash Mixtures with the Use of Limestone:  
9 Improving Constructability for Sustainability

10  
11  
12  
13  
14  
15  
16  
17  
18 Submission Date: 06 February 2012  
19 Word Count: 5200 words, 8 figures and tables

20  
21  
22  
23 Authors:

24  
25 Lisa R. Gurney  
26 Engineering Laboratory  
27 National Institute of Standards and Technology  
28 Gaithersburg, MD 20899 USA  
29 E-mail: [lgurney@et.byu.edu](mailto:lgurney@et.byu.edu)

30  
31 Dale P. Bentz  
32 Engineering Laboratory  
33 National Institute of Standards and Technology  
34 Gaithersburg, MD 20899 USA  
35 E-mail: [dale.bentz@nist.gov](mailto:dale.bentz@nist.gov)  
36 (Corresponding author)

37  
38 Taijiro Sato  
39 National Research Council Canada  
40 Ottawa, Ontario K1A 0R6 Canada  
41 E-mail: [taijiro.sato@nrc-cnrc.gc.ca](mailto:taijiro.sato@nrc-cnrc.gc.ca)

42  
43 W. Jason Weiss  
44 Purdue University  
45 West Lafayette, IN 47907 USA  
46 E-mail: [wjweiss@purdue.edu](mailto:wjweiss@purdue.edu)  
47

48 **ABSTRACT**

49 From a sustainability perspective, high volume fly ash (HVFA) concretes are attractive not only  
50 because of the reduction in cement content and its associated greenhouse gases that they provide,  
51 but also because they avoid landfilling excessive quantities of fly ash. These sustainability  
52 benefits are often tempered by practical constructability limitations that may exist for HVFA  
53 concretes: retardation and diminution of the early age reactions, delays in setting (and finishing  
54 operations), and lower early-age strengths. This paper explores the alleviation of these  
55 deficiencies in HVFA mixtures via the incorporation of fine limestone powders into ternary  
56 blends. Isothermal calorimetry and Vicat needle penetration measurements are employed to  
57 assess reaction rates and setting times, respectively. A systematic variation of the content and  
58 fineness of the limestone powder in mixtures containing either a Class C or a Class F fly ash  
59 indicates that setting times are linearly correlated with the surface area supplied by the limestone.  
60 Comparison of a limestone system to one containing an inert  $\text{TiO}_2$  of similar particle size  
61 indicates that the acceleration and amplification effects of the limestone are due to both physical  
62 (nucleation) and chemical (additional calcium ions) processes. The results indicate that ternary  
63 blends with 40 % of the cement by volume replaced by 30 % to 35 % fly ash and 5 % to 10 %  
64 limestone at a constant water volume fraction can be achieved without significant delays in  
65 setting.

## 66 INTRODUCTION

67 The sustainability movement has renewed interest in reducing the cement content in concrete  
68 mixtures in an effort to reduce the carbon footprint of concrete manufacturing and to reduce  
69 production costs. One approach is to decrease the amount of portland cement in concrete by  
70 replacing a percentage of it with supplementary cementitious materials (SCMs). Fly ash, a  
71 byproduct of coal combustion, is a commonly used SCM, yet a large portion of it still ends up in  
72 landfills. By utilizing blended cements containing fly ash, not only can manufacturing costs be  
73 lowered, but landfill disposal can also be reduced.

74 Blended cement concretes that contain high volumes of fly ash (HVFA- typically 35 % to  
75 60 % of the cement is replaced with fly ash) have shown attributes similar or superior to 100 %  
76 cement mixtures at late ages. However, these HVFA mixtures often exhibit retardation of  
77 reactions, low early-age strengths, and delayed setting times. Thus, the perceived potential  
78 sustainability of HVFA mixtures is often not realized since these mixtures are not implemented  
79 due to their lack of constructability [1]. These significant delays in setting are partially due to a  
80 dilution effect of having less of the reactive cement and are sometimes compounded by chemical  
81 incompatibilities between the fly ash and cement that retard or otherwise modify hydration  
82 behavior of the cement. Limestone powders have also been investigated for use as SCMs and  
83 have shown slightly increased early-age compressive strengths [2, 3] and accelerated hydration  
84 rates [2, 4]. Studies have indicated that finer particles generally yield shorter set times and  
85 accelerated hydration in blended cements [3, 5]. Kadri et al. [2] observed that additions of very  
86 finely ground silica fume, alumina or limestone increase the rate of hydration heat development  
87 and early-age compressive strength, but of these three, limestone had by far the greatest effect.  
88 Kadri et al. [2] and De Weerd et al. [6] attributed this acceleration to both limestone's particle  
89 size (nucleation sites) and its chemical nature.

90 Other studies conducted to explore the behavior of cement – fly ash – limestone ternary  
91 blends compared to binary blends, show greater compressive strength and a partial alleviation of  
92 the negative effects observed in cement – fly ash mixtures [3, 6]. It has been further  
93 demonstrated that the beneficial effects of limestone additions observed in pure portland cement  
94 systems are amplified in the presence of fly ash [6, 7]. The objective of the current study is to  
95 determine whether limestone can reduce delays in setting. Further, this work will establish  
96 quantitative relationships between initial and final setting times of ternary mixtures and the total  
97 surface area provided by the limestone powder, for cement blended with either a Class C or a  
98 Class F fly ash.

99

## 100 MATERIALS AND EXPERIMENTAL METHODS

101 This study was conducted using Type I/II ordinary portland cement (OPC - ASTM C150 [8]).  
102 Two cements from the same manufacturer were obtained at different times and have slightly  
103 differing characteristics: the first was used with the Class C (ASTM C618-08a [9]) fly ash  
104 mixtures and the second with the Class F fly ash mixtures. Their respective Blaine fineness  
105 values are 367 m<sup>2</sup>/kg and 383 m<sup>2</sup>/kg, with estimated Bogue potential phase compositions of 52 %  
106 C<sub>3</sub>S, 17 % C<sub>2</sub>S, 8 % C<sub>3</sub>A, and 10 % C<sub>4</sub>AF for sample 1; and 51 % C<sub>3</sub>S, 18 % C<sub>2</sub>S, 7 % C<sub>3</sub>A, and  
107 11 % C<sub>4</sub>AF by mass for sample 2, respectively. Both Class C and Class F fly ashes were  
108 considered because of their generally different behaviors when combined with OPC. The  
109 specific gravity and chemical composition of the OPCs and fly ashes are provided in Table 1.  
110 The Class C fly ash has a fairly high calcium oxide content of 24.63 % and is reactive with  
111 water. Both fly ashes have specific gravities that are lower than that of the OPCs, with the

112 Class F fly ash specific gravity being only about 70 % of the OPC value. While the Class C fly  
113 ash is of a size similar to that of the OPC, the Class F fly ash is significantly coarser, as  
114 exemplified by its higher  $d_{10}$ ,  $d_{50}$ , and  $d_{90}$  (e.g., the diameter below which 90 % of the particles  
115 are found) values in Table 1. The Class C fly ash was specifically selected for this study based  
116 on its known incompatibilities and tendency to retard reactions [10].

117 Shown in Table 2 are the characteristics of the five limestone powders, four from the  
118 same manufacturer having median particle diameters of 17  $\mu\text{m}$ , 3  $\mu\text{m}$ , 1.4  $\mu\text{m}$ , and 0.7  $\mu\text{m}$ , and a  
119 nanoparticle-sized limestone obtained from a separate source. The median diameters of the  
120 micron-sized limestones are those reported by the manufacturer, while the size of the nano-  
121 limestone was obtained through microscopy techniques and reported to be in the range of 50 nm  
122 to 120 nm [11]. BET (Brunauer, Emmett, and Teller [12]) techniques using nitrogen adsorption  
123 were employed to obtain the surface area of each of the five limestones. Also in this study, a  
124 fine anatase ( $\text{TiO}_2$ ), having a specific gravity of 3.9, a median diameter of 0.7  $\mu\text{m}$ , and a BET  
125 surface area of 10.12  $\text{m}^2/\text{g}$  was used as a chemically inert fine particle to examine if it could  
126 provide physical surfaces for the nucleation and growth of hydration products.

127 The cement pastes were designed to maintain constant volume fractions of water and  
128 powders, based on a control mixture with a water-to-cement ratio ( $w/c$ ) of 0.35 by mass.  
129 Constant volumetric proportions were maintained to provide the fairest comparison of setting  
130 times. The nominal goal of the investigated mixtures was to replace 40 % of the cement by  
131 volume with other powders (fly ash or limestone). The design of each mixture and its  
132 corresponding  $w/c$  and water-to-cementitious material ratios ( $w/cm$ ) by mass are provided in  
133 Table 3. Cement, fly ash, and limestone are all considered as cementitious materials in  
134 computing  $w/cm$ . Subsequently, any reference to a particular sample will refer to the ratio of its  
135 constituent materials. For example, a sample that contains volume percentages of 55 % cement  
136 powder, 40 % Class F fly ash and 5 % limestone with a 1.4  $\mu\text{m}$  diameter will be referenced as  
137 “55-40F-5@1.4 $\mu\text{m}$ .” The ratios chosen in this experiment were selected based on some  
138 preliminary lab work to investigate the optimal blends of OPC, fly ash, and limestone. No water  
139 reducing admixtures were used in this study, to avoid any confounding of their influence on  
140 hydration and setting with that of the powder materials. However, a recent study of  
141 cement/SCM/limestone ternary blends employing a high range water reducer has obtained results  
142 similar to those achieved in the present work [13].

143 Each mixture was individually prepared by first pre-blending the dry ingredients for  
144 30 min in a powder blender, then mixing them with water in a high shear blender following the  
145 procedure developed by the Portland Cement Association [14]. After mixing, the paste was put  
146 into a truncated conical specimen for evaluation of setting times using the Vicat needle, and a  
147 small amount of the prepared material was placed in a glass vial for measurement of heat release  
148 using isothermal calorimetry.

149 The Vicat needle penetration tests were conducted according to the ASTM C191  
150 standard [15], but with the following modifications. First, to minimize evaporation from the  
151 specimen surface during the course of the test, a moist sponge was held in place in the bottom of  
152 a foam cup using toothpicks, and the inverted cup placed on top of the truncated conical cement  
153 paste specimen in an effort to maintain a near 100 % relative humidity environment surrounding  
154 the hardening cement paste. The cup was removed prior to each measurement and returned  
155 immediately after recording the needle penetration. The second modification was to redefine  
156 “final set” to be the time at which the Vicat needle penetrates no more than 1 mm into the paste.  
157 Some of the Vicat specimens exhibited excessive bleeding and although the needle would not

158 penetrate, it would continue to leave a mark on the surface for many hours as the bleed water  
159 was slowly reabsorbed. In the ASTM C191 standard [15], the single laboratory precisions are  
160 listed as 12 min (0.2 h) and 20 min (0.33 h) for the initial and final times of setting, respectively.  
161 All set time measurements were conducted inside a walk-in environmental chamber maintained  
162 at  $(25.0 \pm 1.0) ^\circ\text{C}$ .

163 Following the general guidelines provided in the ASTM C1702 standard [16], isothermal  
164 calorimetry was conducted for a period of at least 24 h, using paste specimens having a mass of  
165 between 4.98 g and 5.26 g. The prepared paste was carefully placed in the glass calorimeter  
166 specimen vials, the vials were sealed, and the sealed vials were then loaded into the calorimeter  
167 along with a reference vial containing only dry cement powder. Using this procedure, the initial  
168 “mixing” peak that occurs when water contacts cement was not examined in this study. For this  
169 technique, the average absolute difference between replicate specimens of cement paste was  
170 measured to be  $3.16 \times 10^{-5}$  W/g (cement), with a maximum absolute difference of  $9.10 \times 10^{-5}$  W/g  
171 (cement), for measurements conducted between 1 h and 24 h after mixing. Calorimetry data was  
172 collected as a quantitative indication of the ongoing reactions and because of its high correlation  
173 with the stiffness and compressive strength of mortars and pastes [3, 17].  
174

## 175 **RESULTS AND DISCUSSIONS**

176 Vicat needle penetration and isothermal calorimetry data for all mixtures are presented and  
177 compared in the following figures and tables. Calorimetry data provides a comparison of the  
178 ongoing reaction rates (acceleration/retardation/amplification/diminution of the heat flow  
179 compared to the 100 % cement paste), while Vicat needle penetration depends on chemical  
180 reaction rates along with the accompanying physical process of building “bridges” between the  
181 cement particles to induce setting.  
182

### 183 **Vicat Results**

184 Figure 1 and Table 4 show the results of the Vicat needle penetration tests for both classes of fly  
185 ash. By definition, the time of a 25 mm penetration of the Vicat needle is the initial set time, as  
186 indicated in each plot by a horizontal dashed line. For the Class C fly ashes, the mixtures  
187 with 5 % limestone are shown in lighter shades and marked with a triangle, while those  
188 with 10 % limestone are in darker shades and marked with a square.

189 The 60-40 fly ash mixtures containing no limestone exhibit the greatest delays in initial  
190 and final set times due to dilution (Class F and Class C) and retardation (Class C) effects. The  
191 lack of retardation in the chemical reactions due to the Class F fly ash is verified by examining  
192 the heat flow curves in Figure 2. The initial set times of these mixtures are delayed from those of  
193 their corresponding control by 3.66 h for the C ash and 0.85 h for the F ash. It is clearly evident  
194 that for both fly ashes examined in this study, an increase in volumetric percentage and/or a  
195 decrease in particle size of limestone reduce the setting times, systematically approaching that of  
196 the control (100 % cement) mixture. Mounanga et al. [3] have similarly observed set  
197 acceleration in ternary mixtures containing fly ash and limestone, noting that the acceleration  
198 was more pronounced with higher limestone contents. Figure 1 indicates that even at a low 5 %  
199 volume fraction, introduction of limestone has an accelerating effect on these ternary blends, but  
200 perhaps more important than the amount of limestone is its particle size. Each progressive  
201 decrease in limestone particle size provides a further decrease in set times, but for the Class C fly  
202 ash mixtures and the limestones examined in this study, a 5 % replacement by volume is not  
203 sufficient to reach the set time of the control. Doubling the amount of limestone significantly  
204 reduces the set time for all sizes of limestone (in the Class C fly ash mixtures), but the best match

205 to the original set time of the control 100 % cement paste is provided by the mixture with 10 %  
206 nano-limestone. For the Class F fly ash mixtures, the 5 % nano-limestone more than adequately  
207 mitigates the delays in set times caused by the 40 % replacement of cement; for this ash, perhaps  
208 a limestone with a diameter between 0.7  $\mu\text{m}$  and 0.12  $\mu\text{m}$  or a smaller amount of the nano-  
209 limestone could be used.

210

### 211 **Calorimetry Results**

212 Showing the heat flow per gram of cement and the cumulative heat release per milliliter of water  
213 for each mixture, Figure 2 uses the same line and marker styles as the Vicat results in Figure 1.  
214 In each plot in Figure 2, the vertical cross marks indicate the initial Vicat set times. The heat  
215 flow plots are scaled per gram of cement to provide an indication of the relative reactivity of the  
216 cement in each mixture, assuming that the fly ashes and limestones are nominally inert during  
217 the first hours of hydration. The cumulative heat release is normalized per volume of water in  
218 each mixture to examine the relationship between heat generation and the filling of this pore  
219 (water) volume with hydration products [17].

220 Type I/II cements typically exhibit a heat flow curve that has two (partially overlapping)  
221 peaks, generally occurring within the first 24 h. The first peak represents reaction of the calcium  
222 silicates, while the second peak (or shoulder in some cases) is generally related to a renewed  
223 period of aluminate reactivity. The effect of a 40 % fly ash replacement on the heat flow curve is  
224 distinct for the representatives of each class of fly ash employed in the current study. The Class  
225 C fly ash introduces a sharp amplification of the second peak, and both peaks are greatly retarded  
226 from those of the control mixture (e.g., by more than 3 h). Conversely the Class F fly ash has a  
227 negligible effect on heat flow and functions mainly as a diluent at early ages.

228 Introducing limestone into the cement-fly ash mixtures does not greatly affect the basic  
229 (two-peak) shape of the heat flow curves, but it does both accelerate and amplify the heat flow,  
230 as observed in previous studies [3, 17]. The observed degree of acceleration and amplification is  
231 greater as the particle size of the limestone decreases, or as the total limestone particle surface  
232 area increases. Cumulative heat data was also collected for the first 24 h after preparing the  
233 mixtures (Table 4), although only the first 10 h is shown in Figure 2. As with the Vicat results,  
234 for the Class C fly ash, the 60-30C-10@nano mixture best reflects the heat of the control mixture  
235 through the first 9 h, but it then drops below the control curve. At an age of 24 h, this nano-  
236 limestone mixture only has 77 % of the cumulative heat release per milliliter of water of the pure  
237 cement mixture; still, it offers the most improvement in 1 d cumulative heat release and therefore  
238 likely in 1 d strength, as has been observed in mortars in a previous study [17]. It is also notable  
239 that all of the mixtures for a given fly ash and a given limestone replacement level have similar  
240 cumulative heat release values at their respective times of initial set.

241

### 242 **Discussion of Findings**

243 Owing to differences in composition, each mixture behaved differently during mixing and  
244 setting. There were some samples that exhibited substantial bleeding; this was most apparent in  
245 the mixtures containing the Class F fly ash, likely due to its lower specific gravity and larger  
246 particle size, an effect that was mitigated with the addition of the finer limestones. While the  
247 mixtures were all designed to have the same volume fraction of water, as they were composed of  
248 various quantities of several materials, they still differed in their observable rheology. Visually,  
249 this correlated to component particle size (as the coarser limestones and fly ashes were less  
250 viscous than their finer counterparts) or equivalently to total particle surface area. The high  
251 viscosities could be reduced through the addition of water reducers, but water reducers were not

252 included in the present study to avoid their confounding influences on hydration and setting.  
253 While the viscosity (and yield stress) varied from one mixture to another, preparing the Vicat and  
254 isothermal calorimetry specimens was readily achievable in every case.

255 Apparent when comparing the results portrayed in Figures 1 and 2, the Vicat tests and  
256 calorimetry data support each other well. The mixtures that best matched the controls in the  
257 Vicat penetration test results in Figure 1 were also the most similar to the 100 % OPC control in  
258 cumulative heat release in Figure 2. For each fly ash at each limestone volume fraction, the  
259 cumulative heat release at initial set was approximately a constant value. Since these mixtures  
260 were all formulated with the same volume fraction of water, one can hypothesize that each would  
261 require a similar volume of hydration product formation to bridge the cement particles and  
262 produce setting. At the same volume fraction of limestone (5 %), the Class C fly ash mixtures  
263 required a greater amount of heat to produce initial setting than the Class F fly ash mixtures.  
264 This is likely due to the additional initial heat provided by the Class C fly ash reacting during the  
265 first few hours, as seen at the far left of the heat flow curves in Figure 2. This particular Class C  
266 fly ash is hydraulic and will flash set when mixed alone with water [17]. In a blended system,  
267 these fly ash reactions contribute heat but apparently don't contribute substantially to building  
268 the necessary bridges between the (floculated) cement particles. For each fly ash, these heat  
269 release values at initial set are substantially higher than those of the control system, as the  
270 addition of fly ash and/or limestone particles dilutes and further separates the remaining cement  
271 particles (higher  $w/c$  in Table 3); naturally, more hydration and its accompanying heat release  
272 would be necessary to achieve setting in this case, similar to an increase in  $w/c$  having minimal  
273 effects on calorimetry but causing noticeable set time delays [18].

274 The 60-35-5@anatase mixtures were useful in distinguishing the cause of the acceleration  
275 and amplification seen in the mixtures containing the same volumetric proportions of limestone,  
276 particularly as the anatase has the same median particle diameter as the 0.7  $\mu\text{m}$  limestone. For  
277 both classes of fly ash, the anatase mixture shows a slight acceleration from the 60-40 mixture in  
278 heat flow, but less so for the Vicat results. This small acceleration may be attributed partially to  
279 the decrease in fly ash concentration that accompanies the addition of the anatase. The other  
280 contribution to this acceleration may be the increased surface area and number of nucleation sites  
281 provided by the finer anatase particles. The anatase mixtures also exhibited higher viscosities, as  
282 would be expected with fine anatase particles replacing coarser fly ash ones. In comparison, the  
283 acceleration/amplification provided by the 1.4  $\mu\text{m}$  limestone is dramatically larger (see also the  
284 24 h heat release values in Table 4), supporting that the limestone plays both physical and  
285 chemical roles in influencing the cement and fly ash reactions at early ages [2, 17]. While  
286  $\text{CaCO}_3$  (limestone) is not very soluble at the higher pHs typical of pore solutions, the initial  
287 contact of the (three) powders is with a fairly neutral pH distilled water [17]. Finer limestone  
288 powders would be expected to dissolve more rapidly during this initial contact, prior to the pH of  
289 the pore solution increasing to over 12 due to concurrent cement (and fly ash) dissolution. In  
290 support of this hypothesis, preliminary measurements of calcium ion concentrations in  
291 centrifuged pore solutions have indeed indicated a higher calcium concentration for a cement-fly  
292 ash paste with a nano-limestone addition vs. one without limestone.

293 The ternary mixture containing Class C fly ash that best reflects the control is the 60-  
294 30C-10@nano mixture; it had an initial set time delay of only 9 min (0.15 h). The best mixture  
295 containing the Class F fly ash would be somewhere between the 0.7  $\mu\text{m}$  and 0.12  $\mu\text{m}$  (nano)  
296 limestone mixtures. An optimal mixture can be achieved by using a limestone with a median  
297 diameter between those two values, or perhaps by slightly reducing the amount of limestone in

298 the nano mixture. It is also evident from the data shown in Figure 1 that decreasing particle size  
 299 from 0.7  $\mu\text{m}$  to 0.12  $\mu\text{m}$  (nano) has a greater accelerating effect than any other decrement (e.g.,  
 300 with the F ash, decreasing from 17  $\mu\text{m}$  to 3  $\mu\text{m}$  and even 1.4  $\mu\text{m}$  had very little effect on the  
 301 initial set time and hydration heat curves). Although throughout this paper, the limestones have  
 302 been referred to by their median particle diameters, it is likely that their surface area better  
 303 constitutes the extent of their acceleration and amplification of hydration. An additional variable  
 304 that could influence this acceleration and amplification is the crystallinity of the limestone; this  
 305 parameter was not assessed in the present study, but could be a topic for future research.

306 Figure 3 explores the relationship between total limestone surface area per unit volume of  
 307 paste and set times. The limestone surface area was calculated based on the mixture proportions  
 308 and the measured BET value for each limestone powder (Table 2). For each individual fly ash at  
 309 each limestone concentration, a linear relationship with a high correlation coefficient ( $R^2$ ) is  
 310 observed for both initial and final set times. Linear relationships with a positive slope and  
 311  $R^2 \geq 0.92$  (not shown) between cumulative heat release at a specific early age (4 h or 8 h for  
 312 example) and surface area provided by the limestone were also observed. Unfortunately,  
 313 whether limestone is providing acceleration and amplification due to its dissolution (chemical) or  
 314 due to providing nucleation sites and additional surface area for the growth of hydration products  
 315 (physical), a linear relationship between surface area and set times (or heat release) would be  
 316 expected. The fact that the data points for anatase included in Figure 3 lie significantly above the  
 317 limestone lines in both cases further supports the hypothesis that at least part of the acceleration  
 318 and amplification produced by the limestone is due to chemical effects.

319 While the plots in Figure 3 do not clearly delineate between the specific mechanisms of  
 320 fine limestone powder acceleration, they do provide a useful tool for estimating the limestone  
 321 surface area that must be provided to each system to mitigate the delayed setting response of a  
 322 high volume fly ash mixture. The procedure to estimate the necessary limestone particle size  
 323 (distribution) for a given set of mixture proportions would be straightforward based on the  
 324 individual lines in Figure 3. To estimate the limestone volume fraction necessary given a  
 325 specific limestone particle size distribution (surface area), one would need to interpolate between  
 326 or extrapolate beyond the lines established for specific volume fractions, as exemplified by the  
 327 two lines for the Class C fly ash in Figure 3. To demonstrate this more clearly, for the Class C  
 328 fly ash mixtures, the initial set time results are plotted against limestone volume fraction in  
 329 Figure 4. For a given limestone, the lines in Figure 4 could be used to estimate the required  
 330 limestone replacement level to provide equivalence (or any desired delay) in initial set time  
 331 relative to that of the control mixture. Thus, a standardized procedure could be to 1) determine  
 332 the set time for a control mixture or that desired for the HVFA mixture, 2) determine the current  
 333 set time for the HVFA mixture, 3) determine the set time for one level of limestone replacement  
 334 (say 5 %), 4) estimate the required limestone replacement level to achieve the desired set time  
 335 using a law of mixtures, and 5) prepare a trial batch with this calculated limestone replacement  
 336 level to verify performance. The law of mixtures would simply provide a linear-based estimate  
 337 of the required limestone replacement level as:

$$338 \quad \% \text{ limestone for desired performance} = \left[ \frac{t_{HVFA} - t_{desired}}{t_{HVFA} - t_{limestone}} \right] * (\% \text{ limestone in test mixture}) \quad (1)$$

340  
 341 where  $t_{HVFA}$  is the set time of the HVFA mixture with no limestone replacement,  $t_{desired}$  is the  
 342 desired set time (e.g., that of the control 100 % OPC mixture), and  $t_{limestone}$  is the measured set



343 time of the mixture with the test level of limestone replacement. This procedure could be  
344 employed for engineering either the initial or the final set times of the ternary blend mixture.  
345

## 346 CONCLUSIONS

347 Based on the materials examined in this study, the following conclusions can be drawn:

- 348 1) fine (on the order of 1  $\mu\text{m}$  median diameter) limestone powder replacement for a portion of  
349 the fly ash in a high volume fly ash mixture is an effective approach to mitigating excessive  
350 delays in setting times,
- 351 2) the performance of the limestone in this respect is related to its surface area (as measured  
352 using BET methods),
- 353 3) a linear relationship exists between the initial and final set times and the surface area provided  
354 by the limestone replacements in each type of ternary mixture,
- 355 4) for a fixed water volume fraction, the cumulative heat release per milliliter of water at initial  
356 set is constant for a given fly ash with a given concentration of limestone replacement, and
- 357 5) each cement/fly ash combination will likely exhibit a unique early-age behavior with some  
358 requiring relatively large additions (10 % or more) of a very fine limestone and others needing  
359 only a minor addition of a coarser limestone powder to adequately mitigate setting time delays.

360 This study has focused on the alleviation of delayed setting times via the addition of fine  
361 limestone powders to HVFA paste mixtures. Other properties such as compressive strength  
362 development and autogenous shrinkage at early ages (since the limestone powders being  
363 employed are quite fine) should be evaluated in the future to establish their relationship to the  
364 characteristics of the limestone powders in mortar/concrete mixtures. The results to date indicate  
365 a promising potential for these ternary mixtures to achieve equivalent performance to 100 %  
366 OPC systems, with substantial cost, energy, and CO<sub>2</sub> footprint reductions, successfully achieving  
367 the joint critical objectives of constructability and sustainability.  
368

## 369 ACKNOWLEDGEMENTS

370 The authors would like to thank Mr. Max Peltz of the Engineering Laboratory at the  
371 National Institute of Standards and Technology (NIST) for his assistance with the experiments  
372 and for performing the BET measurements. They would also like to acknowledge the provision  
373 of materials by Lafarge, Lehigh Cement Corporation, OMYA, and Separation Technologies,  
374 LLC. Lisa R. Gurney would like to thank the NIST Summer Undergraduate Research  
375 Fellowship (SURF) program for providing her the opportunity to work on this project.  
376

## 377 REFERENCES

- 378 1) Cost, V.T. Concrete Sustainability Versus Constructability – Closing the Gap, 2011  
379 International Concrete Sustainability Conference, Boston, 2011.
- 380 2) Kadri E.H., S. Aggoun, G. De Schutter, and K. Ezziane. Combined Effect of Chemical  
381 Nature and Fineness of Mineral Powders on Portland Cement Hydration. *Materials and*  
382 *Structures*, Vol. 43, No. 5, 2009, pp. 665-673.
- 383 3) Mounanga P., M.I.A. Khokhar, R. El Hachem, and A. Loukili. Improvement of the  
384 Early-Age Reactivity of Fly Ash and Blast Furnace Slag Cementitious Systems Using  
385 Limestone Filler. *Materials and Structures*, Vol. 44, 2011, pp. 437-453.
- 386 4) Menendez G., V. Bonavetti, and E.F. Irassar. Strength Development of Ternary Blended  
387 Cement with Limestone Filler and Blast-Furnace Slag. *Cement and Concrete Composites*,  
388 Vol. 25, No. 1, 2003, pp. 61-67

- 389 5) Quian J., C. Shi, and Z. Wang. Activation of Blended Cements Containing Fly Ash.  
390 *Cement and Concrete Research*, Vol. 31, No. 8, 2001, pp.1121-1127.
- 391 6) De Weerd K., M. Ben Haha, G. Le Saout, K.O. Kjellsen, H. Justnes, and B. Lothenbach.  
392 Hydration Mechanisms of Ternary Portland Cements Containing Limestone Powder and  
393 Fly Ash. *Cement and Concrete Research*, Vol. 41, 2011, pp. 279-291.
- 394 7) De Weerd K., K.O. Kjellsen, E. Sellevold, and H. Justnes. Synergy Between Fly Ash  
395 and Limestone Powder in Ternary Cements. *Cement and Concrete Composites*, Vol. 33,  
396 No. 1, 2010, pp. 30-38.
- 397 8) ASTM C150. Standard Specification for Portland Cement; 2009.
- 398 9) ASTM C618-08a. Standard Specification for Coal Fly Ash and Raw or Calcined Natural  
399 Pozzolan for Use in Concrete. 2008
- 400 10) Bentz D.P., C.F. Ferraris, I. De la Varga, M.A. Peltz, and J. Winpigler. Mixture  
401 Proportioning Options for Improving High Volume Fly Ash Concretes. *International*  
402 *Journal of Pavement Research and Technology*, Vol. 3, No. 5, 2010, pp. 234-240.
- 403 11) Sato T., and J. Beaudoin. Effect of Nano-CaCO<sub>3</sub> on Hydration of Cement Containing  
404 Supplementary Cementitious Materials. *Advances in Cement Research*, Vol. 23, No. 1,  
405 2011, pp. 1-11.
- 406 12) Brunauer, S., P.H. Emmett, and E. Teller. Adsorption of Gases in Multimolecular Layers.  
407 *Journal of the American Chemical Society*, Vol. 60, 1938, 309-319.
- 408 13) Cost, T. Optimization of Concrete Paving Mixtures for Sustainability and Performance.  
409 Submitted to the International Conference on Concrete Pavements, 2012.
- 410 14) Helmuth R.A., L.M. Hills, D.A. Whiting, and S. Bhattacharja. Abnormal Concrete  
411 Performance in the Presence of Admixtures. 1995 PCA serial # 2006.
- 412 15) ASTM C191-08. Standard Test methods for Time of Setting of Hydraulic Cement by  
413 Vicat Needle. 2008.
- 414 16) ASTM C1702-09a. Standard Test Method for Measurement of Heat of Hydration of  
415 Hydraulic Cementitious Materials Using Isothermal Conduction Calorimetry. 2009.
- 416 17) Bentz D.P., T. Sato, I. De la Varga, and J. Weiss. Fine Limestone Additions to Regulate  
417 Setting in High Volume Fly Ash Mixtures. *Cement and Concrete Composites*, Vol. 34,  
418 No. 1, 2012, pp. 11-17.
- 419 18) Bentz, D.P., M.A. Peltz, and J. Winpigler. Early-Age Properties of Cement-Based  
420 Materials: II. Influence of Water-to-Cement Ratio. *ASCE Journal of Materials in Civil*  
421 *Engineering*, Vol. 21, No. 9, 2009, pp. 512-517.
- 422

## 423 List of Tables

424

425 TABLE 1 Oxide Composition Percent by Mass and Physical Characteristics of the Cement and  
426 Fly Ashes

427

428 TABLE 2 Calcium and Magnesium Carbonate Contents, Median Diameters, Specific Gravities  
429 and Measured Surface Areas of the Five Limestones Investigated

430

431 TABLE 3 Percentages by Volume of Cement, Fly Ash and Limestone for Each Mixture and  
432 their Respective  $w/c$  and  $w/cm$

433

434 TABLE 4 Set Times and Cumulative Heat per Milliliter of Water at the Initial Set, Final Set and  
435 24 Hours for Each Mixture

436

## 437 List of Figures

438

439 FIGURE 1 Vicat results for a) Class C and b) Class F fly ash ternary mixtures.

440

441 FIGURE 2 Heat flow and cumulative heat for a) the Class C and b) the Class F fly ash ternary  
442 mixtures. The short vertical lines indicate times of initial set.

443

444 FIGURE 3 Correlation between initial (top) and final (bottom) setting times and surface areas of  
445 the accelerators (powders).

446

447 FIGURE 4 Relationship between initial setting times and limestone replacement level for Class  
448 C fly ash mixtures. The dashed horizontal line indicates the (desired) initial set time of the  
449 control 100 % OPC mixture.

450

451 **TABLE 1 Oxide Composition Percent by Mass and Physical Characteristics of the Cement**  
 452 **and Fly Ashes**

	<b>Cement Sample 1</b>	<b>Class C</b>	<b>Cement Sample 2</b>	<b>Class F</b>
	<b>ASTM C150 I/II</b>	<b>Fly Ash</b>	<b>ASTM C150 I/II</b>	<b>Fly Ash</b>
SiO <sub>2</sub>	19.51	38.38	19.40	59.73
Al <sub>2</sub> O <sub>3</sub>	4.86	18.72	4.86	30.18
Fe <sub>2</sub> O <sub>3</sub>	3.15	5.06	3.62	2.80
CaO	61.76	24.63	61.22	0.73
MgO	3.61	5.08	4.22	0.83
SO <sub>3</sub>	3.12	1.37	3.11	0.02
CO <sub>2</sub>	0.95	-	1.71	-
Alkalies (equivalent)	0.48	-	0.45	-
Insoluble Residue	0.18	-	0.11	-
Na <sub>2</sub> O	-	1.71	-	0.24
K <sub>2</sub> O	-	0.56	-	2.42
Loss on ignition	2.33	0.26	2.55	0.79
Specific gravity	3.15	2.63	3.15	2.16
d (10 %)	1.36 μm	0.85 μm	1.73 μm	3.23 μm
d (50 %)	11.49 μm	10.30 μm	11.83 μm	25.34 μm
d (90 %)	32.67 μm	69.37 μm	35.50 μm	99.06 μm

453

454

455 **TABLE 2 Calcium and Magnesium Carbonate Contents, Median Diameters, Specific**  
 456 **Gravities and Measured Surface Areas of the Five Limestones Investigated**

	<b>17 <math>\mu\text{m}</math></b>	<b>3 <math>\mu\text{m}</math></b>	<b>1.4 <math>\mu\text{m}</math></b>	<b>0.7 <math>\mu\text{m}</math></b>	<b>nano</b>
CaCO <sub>3</sub>	95	96	98	98	> 98
MgCO <sub>3</sub>	2	2	1	1	negligible
Median diameter ( $\mu\text{m}$ )	17	3	1.4	0.7	0.05 to 0.12
Specific gravity	2.71	2.71	2.70	2.70	2.70
BET surface area (m <sup>2</sup> /g)	0.831	2.42	7.06 (0.14) <sup>A</sup>	9.93	19.4

457 <sup>A</sup>Standard deviation amongst three replicate specimens for this limestone.

458

459

460 **TABLE 3 Percentages by Volume of Cement, Fly Ash and Limestone for Each Mixture**  
 461 **and their Respective  $w/c$  and  $w/cm$**

<b>Ternary Mixtures with Class C Fly Ash</b>					
<b>Cement</b>	<b>Fly Ash</b>	<b>Limestone</b>		<b><math>w/c</math></b>	<b><math>w/cm</math></b>
		<b>%</b>	<b>Size</b>		
100	-	-	-	0.350	0.350
60	40	-	-	0.583	0.375
60	35	(5 % TiO <sub>2</sub> )		0.583	0.367
60	35	5	3.0 $\mu\text{m}$	0.583	0.374
60	35	5	1.4 $\mu\text{m}$	0.583	0.374
60	35	5	0.7 $\mu\text{m}$	0.583	0.374
60	35	5	nano	0.583	0.374
60	30	10	1.4 $\mu\text{m}$	0.583	0.374
60	30	10	0.7 $\mu\text{m}$	0.583	0.374
60	30	10	nano	0.583	0.374
<b>Ternary Mixtures with Class F Fly Ash</b>					
<b>Cement</b>	<b>Fly Ash</b>	<b>Limestone</b>		<b><math>w/c</math></b>	<b><math>w/cm</math></b>
		<b>%</b>	<b>Size</b>		
100	-	-	-	0.350	0.350
60	40	-	-	0.583	0.400
60	35	(5 % TiO <sub>2</sub> )		0.583	0.388
60	35	5	17 $\mu\text{m}$	0.583	0.396
60	35	5	3.0 $\mu\text{m}$	0.583	0.396
60	35	5	1.4 $\mu\text{m}$	0.583	0.396
60	35	5	0.7 $\mu\text{m}$	0.583	0.396
60	35	5	nano	0.583	0.396

462

463

464 **TABLE 4 Set Times and Cumulative Heat per Milliliter of Water at the Initial Set, Final**  
 465 **Set and 24 Hours for Each Mixture**

<b>Class C Fly Ash</b>							
	<b>Initial Set Time (h)</b>	<b>Delay from control (h)</b>	<b>Final Set Time<sup>B</sup> (h)</b>	<b>Delay from control (h)</b>	<b>Cumulative Heat (J/mL water)</b>		
					<b>at initial set</b>	<b>at final set</b>	<b>at 24 h</b>
100-0-0	3.39	-	5.26	-	36.0	100.2	570.2
60-40C-0	7.05	3.66	> 8.76	> 3.50	54.1	> 91.3	384.5
60-35C-5@anatase	6.97	3.58	7.52	2.26	52.3	63.5	394.8
60-35C-5@3.0 $\mu\text{m}$	6.36	2.97	8.02	2.76	50.2	85.7	390.0
60-35C-5@1.4 $\mu\text{m}$	6.08	2.69	7.75	2.49	55.2	96.8	407.5
60-35C-5@0.7 $\mu\text{m}$	5.75	2.36	7.00	1.74	55.4	87.6	415.4
60-35C-5@nano	4.97	1.58	6.48	1.23	57.7	97.9	419.7
60-30C-10@1.4 $\mu\text{m}$	4.76	1.36	5.78	0.52	45.5	72.3	429.5
60-30C-10@0.7 $\mu\text{m}$	4.57	1.18	5.50	0.24	43.5	68.0	434.7
60-30C-10@nano	3.54	0.15	4.25	-1.01	44.2	65.1	440.1
<b>Class F Fly Ash</b>							
	<b>Initial Set Time (h)</b>	<b>Delay from control (h)</b>	<b>Final Set Time<sup>B</sup> (h)</b>	<b>Delay from control (h)</b>	<b>Cumulative Heat (J/mL water)</b>		
					<b>at initial set</b>	<b>at final set</b>	<b>at 24 h</b>
100-0-0	3.22	-	4.25	-	30.7	70.6	636.7
60-40F-0	4.07	0.85	6.25	2.00	39.5	107.9	421.8
60-35F-5@anatase	4.29	1.07	5.25	1.00	37.5	65.7	445.9
60-35F-5@17 $\mu\text{m}$	3.83	0.61	5.75	1.50	43.5	106.3	427.3
60-35F-5@3.0 $\mu\text{m}$	3.57	0.35	4.88	0.63	40.2	81.1	433.3
60-35F-5@1.4 $\mu\text{m}$	3.66	0.44	5.00	0.75	46.6	93.7	449.7
60-35F-5@0.7 $\mu\text{m}$	3.40	0.18	4.50	0.25	43.3	82.6	453.8
60-35F-5@nano	3.04	-0.18	3.75	-0.50	45.1	70.3	461.1

466 <sup>B</sup> In this study, “final set” is defined as the time when the penetration of the Vicat needle is less  
 467 than or equal to 1 mm.  
 468

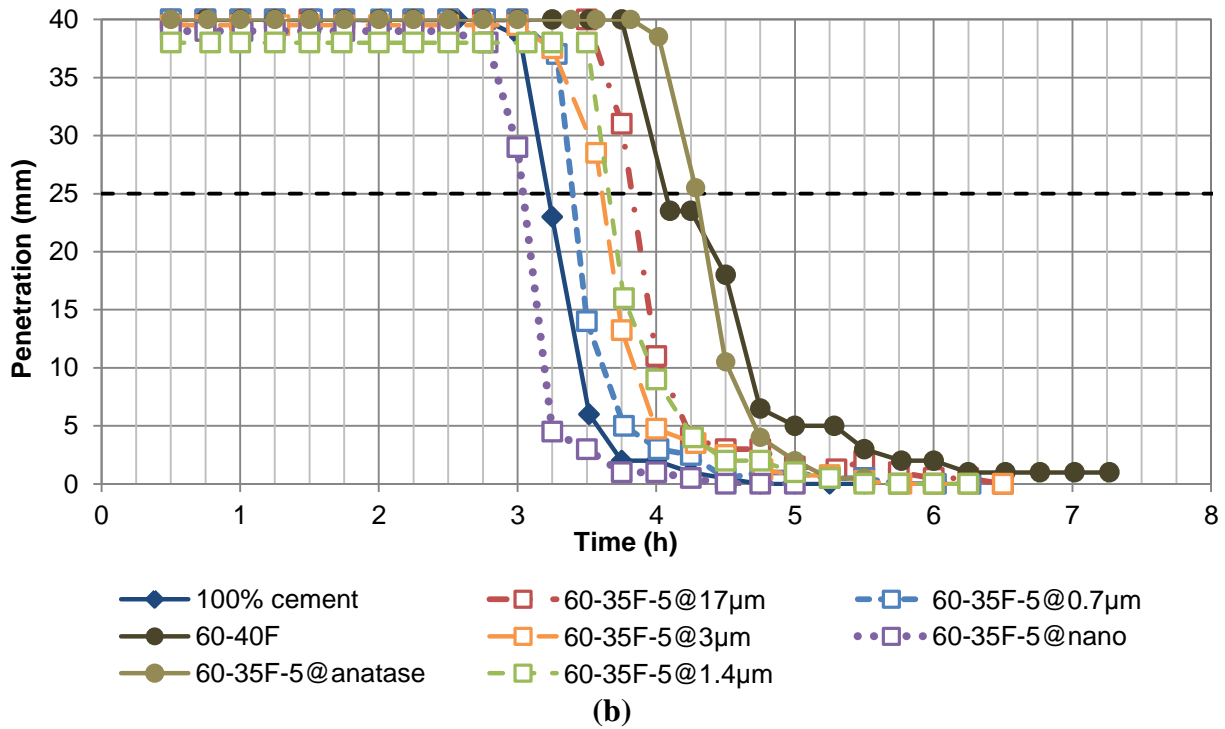
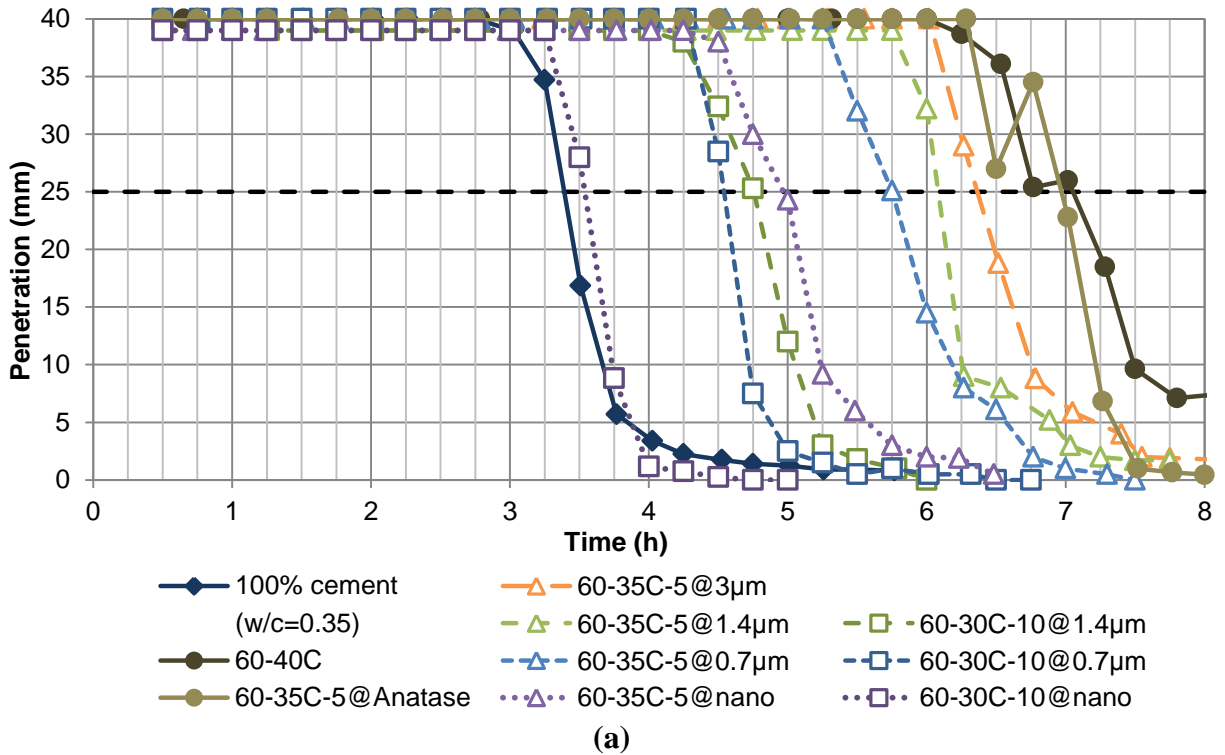
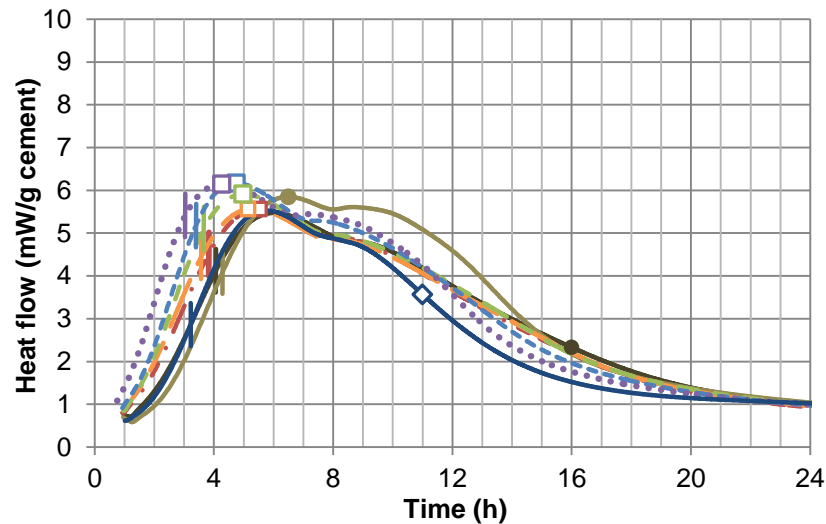
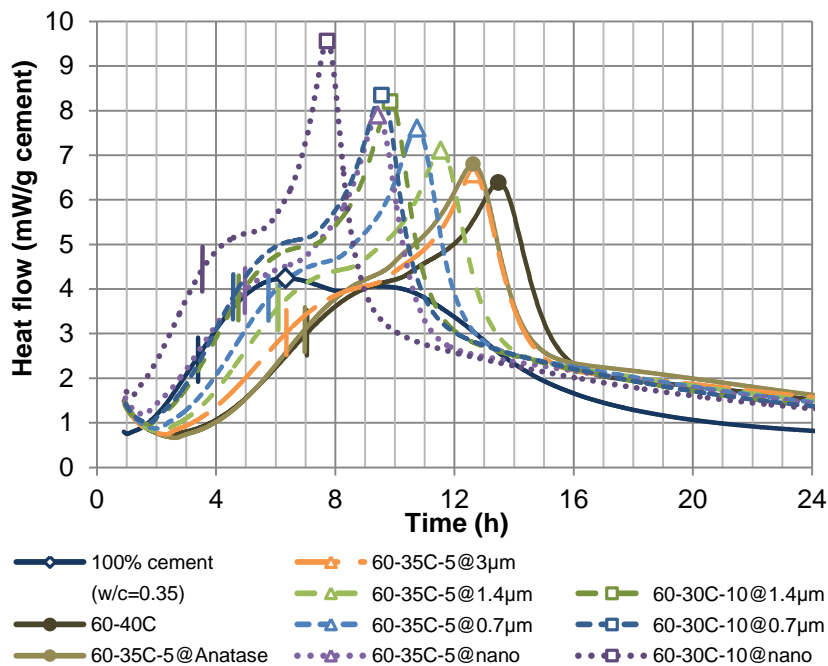
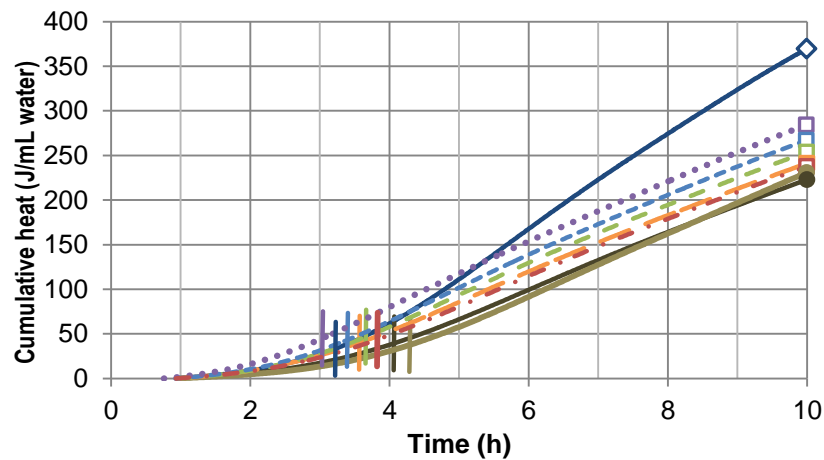
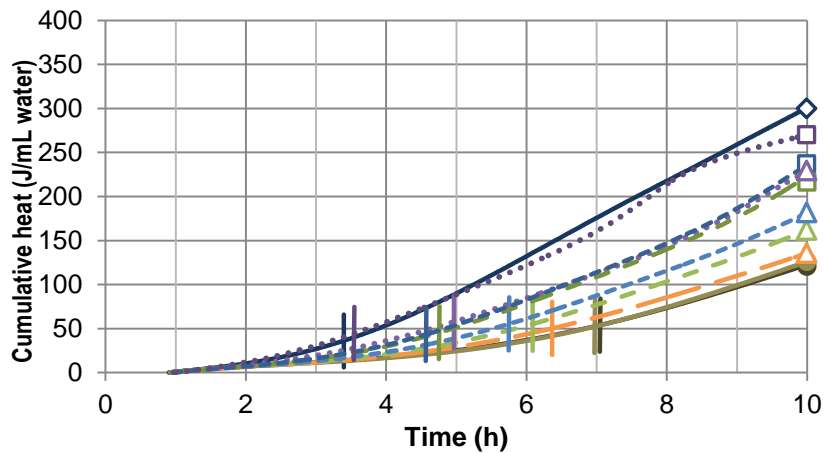


FIGURE 1 Vicat results for a) Class C and b) Class F fly ash ternary mixtures.





476



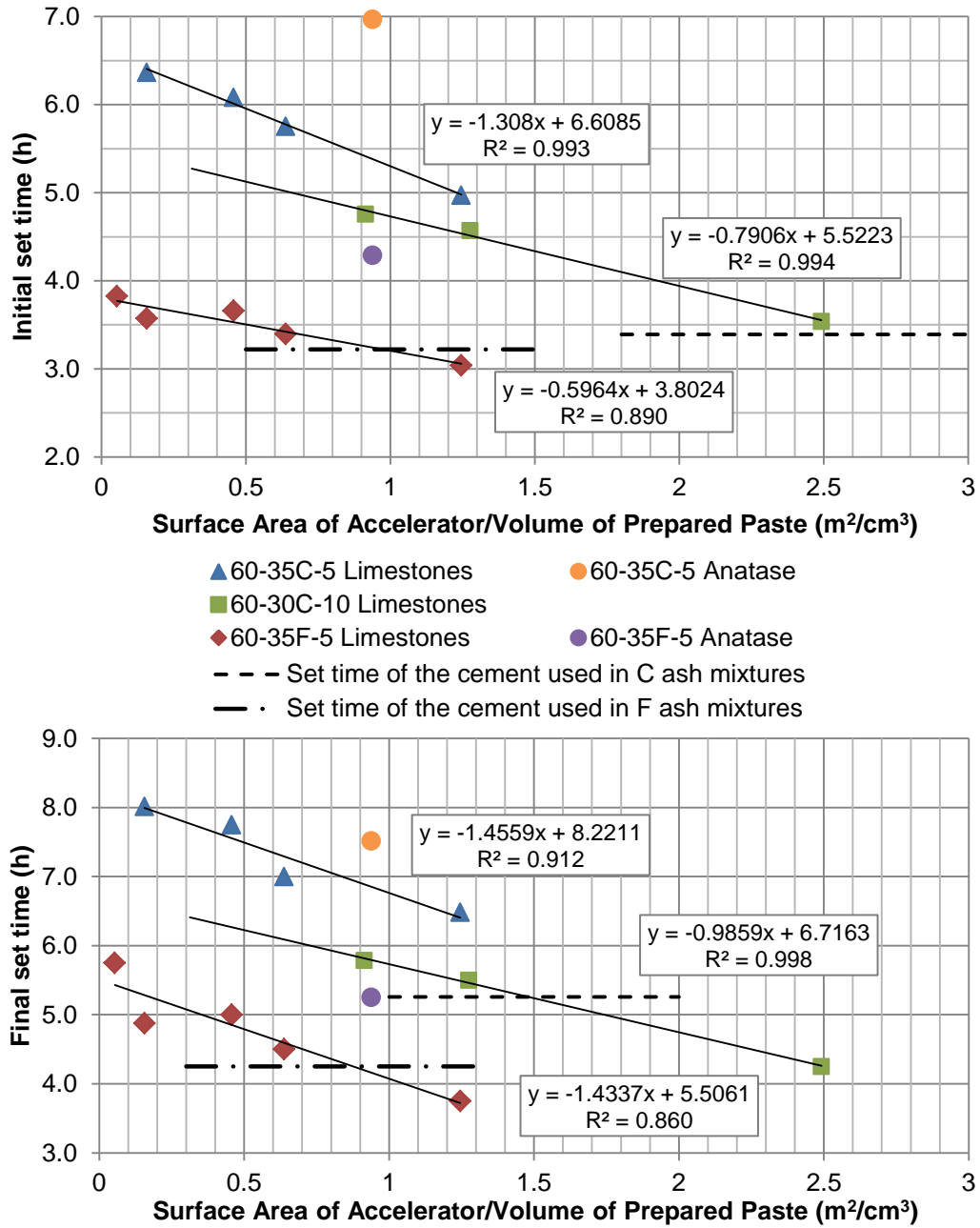
477

478

479

480

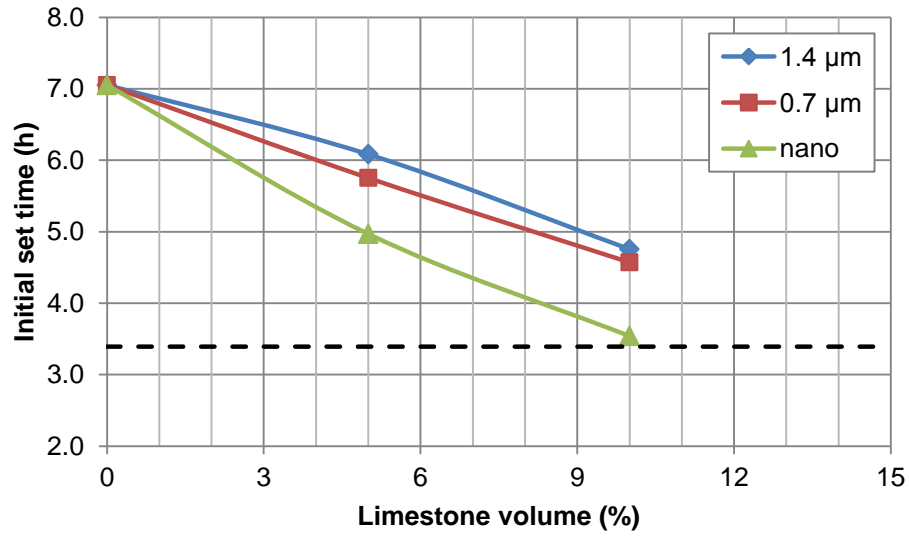
**FIGURE 2** Heat flow and cumulative heat for a) the Class C and b) the Class F fly ash ternary mixtures. The short vertical lines indicate times of initial set.



481

482  
483  
484  
485

**FIGURE 3** Correlation between initial (top) and final (bottom) setting times and surface areas of the accelerators (powders).



486  
487  
488  
489  
490

**FIGURE 4 Relationship between initial setting times and limestone replacement level for Class C fly ash mixtures. The dashed horizontal line indicates the (desired) initial set time of the control 100 % OPC mixture.**